

Study of the stopping target CCD pulse fitting analysis
James S Frank
E949 Tech Note K045
February 9, 2005 version.

One of the important tools that has been used in previous analyses of pnn2 in E787 has been the use of pulse shape fitting in the CCD system analyzing pulse shapes from fibers in the stopping target. I have examined several aspects of this using the pulse fitting parameters in E949 data. A new technique of obtaining a 'tagged' sample is described which allows a calibration of both the absolute efficiency of the pulse fit as a function of second pulse energy as well as a measure of the number of false-positives. By using this technique, a list of cuts is suggested. This 'tagged' method was used to check on the CCD performance in fibers selected without using tags, and the success of this check allowed efficiencies to be determined for fitting pulses in the high-gain CCDs.

Introduction

The CCD system is used to record pulse shapes at 500 MHz over a 256 or 512 ns wide window with 8 bits of dynamic range per point. The scintillating fiber target (TT) is where the K^+ s come to rest and subsequently decay. There are 413 individual fibers $\sim 5\text{mm} \times 5\text{mm}$ square, each coupled to a photomultiplier tube. The instrumentation must be sensitive to a very wide dynamic range of energies: Stopping kaons can deposit up to ~ 100 MeV in an individual fiber, whereas the decay products typically deposit ~ 1 MeV crossing an individual fiber, and may deposit much less if a particle traverses a fiber near a corner. Furthermore, the scintillator plastic is Bicron BCF-92, a fast blue scintillator with a mean decay time of its fast component $\sim 2.5\text{ns}$, and the photomultiplier tubes are Hamamatsu 1635-O2, with a rise time of 0.8ns . Additional instrumentation and cabling change the characteristics so that much of a pulse rises and falls in a total of $\sim 20\text{-}40\text{ns}$.

In order to cover this wide dynamic range, each target element is viewed by 2 separate CCD channels: the 'high-gain' channels view the pulses from each fiber individually; the 'low-gain' channels view the sum of 4 to 6 fibers that are randomly positioned in the TT. The ratio of the gains is about a factor of 3. The high-gain channels are sensitive to pulses with minimum energy of ~ 0.8 MeV, and typically saturate at ~ 25 MeV; the low-gain channels have a threshold and typical saturation about a factor of 3 higher.

The primary functions of the CCD system on the TT are to measure the signal time accurately and to be sensitive to the presence of multiple particles which may pass through each fiber. Indeed, a very important background in the pnn2 analysis occurs when a kaon comes to rest, and decays to a $\pi^+\pi^0$ in which the π^+ is emitted nearly aligned with the beam direction. The π^+ might traverse a short distance in the fiber, undergo an inelastic nuclear reaction, and change its direction before entering the UTC and range stack. For this problematical type of event, the π^0 may be directed mostly due upstream or downstream. The most probable direction for its emitted high-energy photon is opposite the π^+ . When the π^+ is emitted along the beam direction, the higher-energy

photons are also preferentially directed along the beam line. These are regions which have lower photon detection efficiency. The correlation of these two processes proved to constitute the largest background to the pnn2 measurement in E787- the expectation was a signal to noise ratio of about 10%. In E949, the photon detectors were augmented significantly, both along the beam direction and beyond the range stack. Since a suppression of this background of a factor of at least a factor of 10 is desired, it would be good to improve the 2nd pulse detection in the CCDs as well.

Changes E787 -> E949

The instrumentation of the TT and the CCD channels viewing the TT was basically unchanged between E787 and E949. The pulse finding and fitting techniques were modified slightly. (See E787 TN 391, and references therein for a description of the E787 pnn2 analysis, and pulse fitting techniques.) As in E787, the pulse shape for each fiber in each of the high-gain and low-gain CCD channels was determined by collecting an ensemble of pulses identified to be kaons in SWATHCCD. These were normalized to unit area, and aligned with a timing granularity of 0.5ns by interpolation (4 times finer than provided by the 500 MHz CCDs), and average shapes were stored. The effects from saturated pulses and outliers in each time bin were removed by determining the average from the peak of a Gaussian fit. The standard deviation of the Gaussian fit of the pulse shape to the standardized pulse shape was also stored in each time bin.

In the E787 analysis, the standard deviation of the normalized pulses at each point was used as the input error at each point. While this may be OK for single pulses, it is not correct when one is trying to model the expected pulse shape of two pulses, each with a unique area and time. For E949, the error input was determined from the data. The form used was $a + b*\sqrt{d_i}$ where d_i is the CCD pulse data (in raw counts) in time bin i . Presumably, the constant a term is related to instrumental noise, whereas the b term scales with the square-root of the number of photoelectrons in the pulse. For 2002 data, an ensemble of pulses was studied to experimentally determine the error parameters:

High gain: $0.74 + 0.69*\sqrt{d_i}$ Low gain: $1.21 + 0.35*\sqrt{d_i}$:

Another change from E787 was that the ‘pulsate’ algorithm for the TT pulses was turned off. This algorithm separated joined pulses into individual pulses based upon a pattern of a dip followed by higher data values. Studies showed that imposing this algorithm made it difficult to understand the pulse fitting. Also, it was less sensitive to real second pulses, and more likely to call random fluctuations second pulses than the fitting procedures.

Tests of Performance (Low Gain CCDs)

The pulse fitting routines are called in PASS2. For each target fiber with ADC energy of more than 3 MeV, both the low-gain and high-gain CCD channels are examined for the presence of a pulse. First a single-pulse fit is attempted; if the probability of a single-pulse is less than 0.25, then a 2-pulse fit is attempted. Note that in the E949 analysis, these fits are done before target event reconstruction is made in SWATHCCD.

In order to understand the performance of the CCD pulse fitting algorithms, a series of SETUP cuts were first imposed on km21 monitor data:

itgqualt=0 (successful SWATHCCD reconstruction with at least one pion fiber);
220<ptot<260 (km2 momentum peak from UTC and target reconstruction);
abs(tk)<3 (kaon time near zero);
t_{pi}-t_k>6 (delayed coincidence 'DELCO' from TT analysis is more than 6ns);
nk_tg>0 (at least one kaon fiber);
nfitfib>0; l_{in}fitfib>0 (at least one pulse-fit done on both high-gain and low-gain target ccds);
indication that there was one and only one incident kaon and no incident pion from Cerenkov counters within +-50ns of the beam gate (see TN# K042 for rationale)

Since we are studying the CCD pulse efficiency and require information if the 'pion' track did or did not go through any given 'kaon' fiber, we want to eliminate events in which the reconstruction was not known well enough. (In the SWATHCCD analysis, the TT information from each fiber is categorized as belonging to the incoming 'kaon' or outgoing 'pion', or into a few other classifications.) Therefore, we imposed a tight cut on the extrapolation of the UTC track into the target in order to eliminate these poorly reconstructed events:

require at least 3 pion fibers; and demand that the extrapolated UTC track pass through ALL of the pion fibers.

After imposing these setup cuts, some probability distributions are shown in Fig. 1. For these plots, some of the kaon fibers are categorized into groups based upon the distance of the fiber from the projected track from the UTC. One group (shown in the top row) contains those kaon fibers at the vertex in which the range of the extrapolated UTC track is at least 4mm. Non-vertex kaon fibers in which the extrapolated range is at least 4mm is shown in the middle row. In the last group (bottom row), the nearest corner of the kaon fiber is at least 5mm from the UTC track. Note that the 2-pulse fitter is called only when the probability for the single pulse is less than 0.25. When the double pulse fitter is not called, the double-fit probability is set to 0.

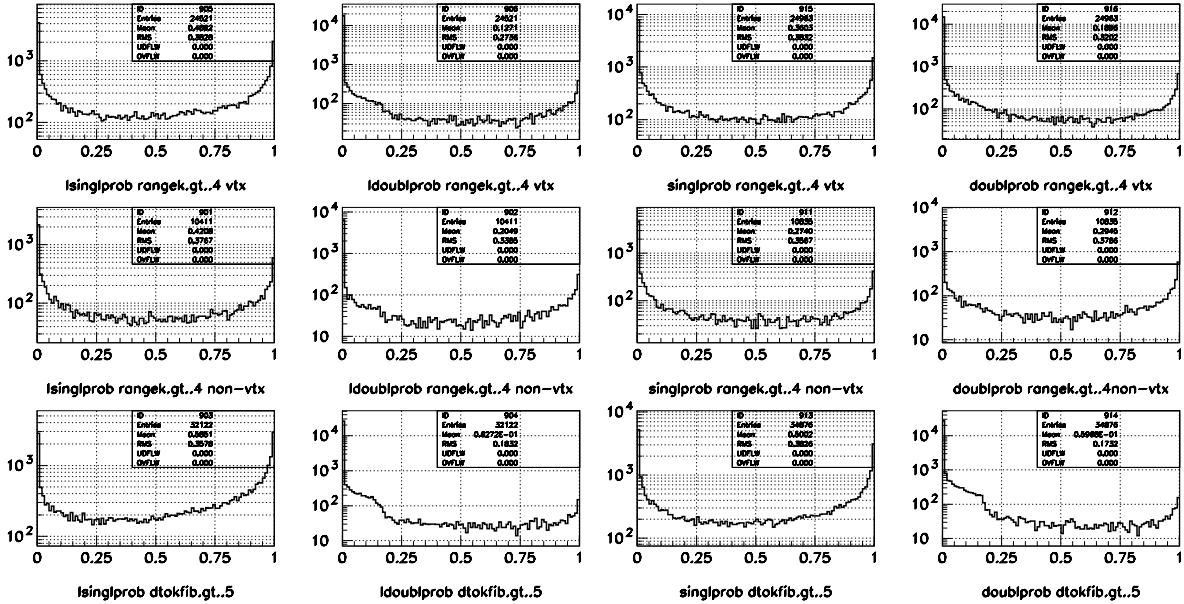


Fig 1a. Low gain single and double fit probability distributions

Fig 1b. High gain single and double fit probability distributions

As might be expected, the probability distributions are different in these three rows. When the UTC track does not go through the fiber (bottom row), the distributions tend to have higher probabilities for single-pulse fits and lower probabilities for double-pulse fits. When the UTC is expected to pass through the fiber, we find lower single-fit probabilities and higher double-fit probabilities. In the vertex fibers (top row), the muon should be created someplace within the fiber, so we expect the true path will be less than the full extrapolated range: the means of the probability distributions are between the other two groups.

Selection of fibers with known second pulses

Now we utilize the fact that the low-gain target CCD channels are multiplexed. In the low-gain CCD channels, we examine those kaon fibers which

- (a) are far from the extrapolated UTC track (the closest corner is $>5\text{mm}$ from the extrapolated UTC track)
- AND
- (b) have a pion found in one of the other fibers that are multiplexed into the same CCD channel containing the kaon. The pion determination was made in SWATHCCD based upon ADC information (non-multiplexed), and time based upon either TDC or high-gain CCD information (also non-multiplexed), but the time is not based in any way upon any low-gain CCD pulse fitting information
- OR
- (b') no pion was found in any of the other fibers that are multiplexed into the same CCD channel containing the kaon.

Predominantly, condition (a) eliminates the vertex fiber and other kaon fibers close to the track in which some unknown amount of pion energy would have likely contributed to the pulse. Condition (b) will be satisfied in those low-gain CCD kaon fibers in which a pion should be contributing to the pulse. To the extent that the event was reconstructed correctly, we then know the energy and time of any second pulse that should follow the kaon hit in the low-gain CCD channels.

In each kaon fiber, we also examine the other fibers multiplexed into the same low-gain CCD unit. In order to eliminate confusion, we do not consider fibers in which opposite-side pions, gammas or nearly-coincident extra activity was found in any of these other fibers. We are left with clean tagged samples in which we know what pulse or pulses went into each low-gain CCD channel. Those in which a kaon and a pion were found (criteria (a) and (b)) give us the correct times and energies that ideally will be found by pulse-fitting in the low-gain CCD channel. Those in which a kaon was found but no pion was found (criteria (a) and (b')) gives us a sample of known fibers in which only a single-pulse should be found. Successful double-pulse fits in this latter category are misidentified (false-positives).

Results of study of low-gain pulse fitting

Provided with these tags, we can then study distributions of various ntuple quantities. The goal of this is to find a set of cuts which is relatively efficient for finding two pulses in fibers that we know have two pulses, and also has a low false-positive probability.

The results of this study are shown in Fig 2 and Fig 3. The cuts used (all low-gain variables) were:

- ldoublprob>0.001 (probability of two-pulse fit >0.001);
- ldoublampp>0 (amplitude of 2nd pulse >0);
- ldoubltimk>-5 (time of 1st pulse>-5ns);
- lnonzbins>2 (number of bins used in fit >2);
- abs(ldoubtimp-ldoubltimk-tpi+tk)<DELCOFITCUT (the difference between the two fit times and the expected time difference < DELCOFITCUT; and
- lsinglprob<ldoublprob/10 (the single fit probability is at least a factor of 10 lower than the double-fit probability).

The efficiency for finding a second pulse in any fiber is shown as a function of DELCO, where DELCOFITCUT was set to 10.

We might expect a variation in efficiency of valid 2 pulse fits as a function of the energies of the two pulses as well as a function of the time-difference between them. We will examine this in a later section.

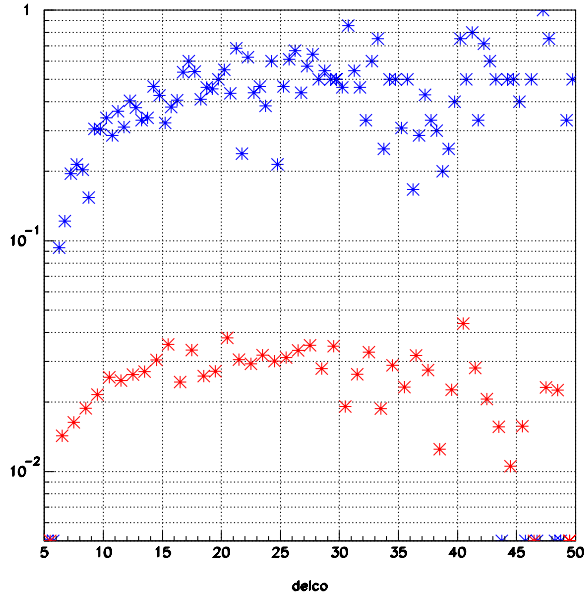


Fig. 2 Pulse finding efficiency as a function of DELCO for low gain CCD channels. The efficiency was plotted in two bins of the known pion energy: blue points have been tagged as having a pion with $\text{epi_tg} > 1.0$ MeV; red points are the ‘false positives’, where $\text{epi_tg} = 0$. The energy of the pion that follows the kaon was tagged by ADC, TDC, and high-gain CCD channels. Cuts are described in the text. This shows that the efficiency of finding a second pulse in the low gain CCDs varies strongly as a function of DELCO. It plateaus approximately after $\text{DELCO} = 15$ ns.

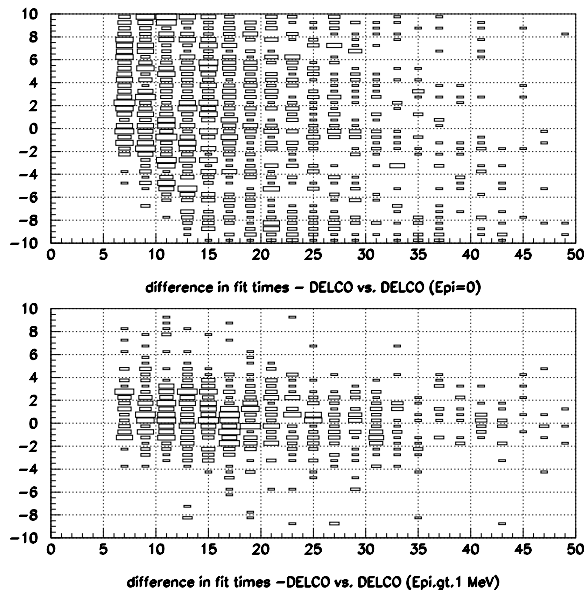


Fig 3. shows two-dimensional histograms of events that passed the above cuts. Plotted is the difference between the fitted times of the two pulses - DELCO vs. DELCO. 1337/53178 events (2.5%) with $\text{epi_tg} = 0$ passed the cuts (top plot). These are false-positives. 734/1957 of the events with $\text{epi_tg} > 1$ MeV passed (38%) the same set of cuts (bottom plot).

We can test other sets of cuts rather easily. For example, in the 1997 pnn2 analysis, the requirement $\text{lsinglprob} > 0.001$ was imposed. Using this cut instead of the cut defined above ($\text{lsinglprob} < \text{ldoublprob}/10$), the efficiency as a function of pion energy and DELCO given in Table 1. (The same 10ns DELCOFITCUT was used in the 1997 analysis. The false probability (pion energy = 0) is about 1/3 of that using the cuts suggested above, but the efficiency is also substantially lower.

One can ‘dial’ a particular acceptance to rejection ratio by modifying DELCOFITCUT. Some results are given in Table 1. ($\text{DELCO} > 15$)

	1997 cuts	New suggested cuts, DELCOFITCUT<10	New suggested cuts, DELCOFITCUT<4
Epi=0 (false positives)	.010	.029	.013
Epi 0 to 0.5 MeV	.025	.071	.034
Epi 0.5 to 1.0 MeV	.074	.171	.132
Epi 1.0 to 1.5 MeV	.138	.375	.309
Epi 1.5 to 3.0 MeV	.386	.628	.602

Table 1. Efficiency of a set of cuts on pulse finding and fitting in the TT for low-gain CCDs at DELCO>15 ns.

It is clear that the suggested cuts are much more efficient in finding valid second pulses in the low-gain CCD channels than the set of cuts used in the 1997 analysis. However, since the errors are being handled differently now, this does not necessarily imply that the pulse fitting efficiency using the new pass2 and the 1997 cuts is the same as one would have gotten using the 1997-pass2 and the 1997 cuts.

Since we know the energy of the two pulses that are merged in the low-gain CCD channels, we can determine how well the energies are actually fit. Fig 4 shows the comparison of the ratios of the calculated pulse areas (from successful two-pulse fits) to the actual pulse energies (from the ADC information).

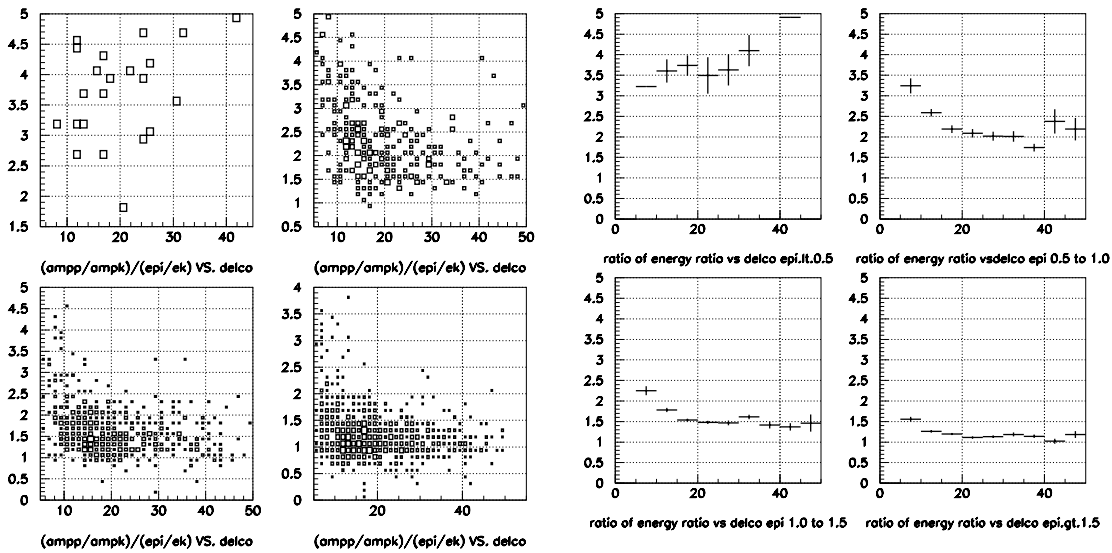


Fig 4. Ratio of calculated pion to kaon energies divided by actual ratio of pion to kaon energies as a function of DELCO in 4 bins of pion energy (<0.5 MeV; 0.5 to 1.0 MeV; 1.0 to 1.5 MeV, >1.5 MeV). The left side shows the 2D histograms; the right side shows the corresponding profile plots.

It is clear that there is a systematic shift in reconstructed pion energies both as a function of DELCO, and as a function of the real energy. The plots show that a ‘1 MeV cut’ on a pion isn’t really discriminating on the real pion energy, at least in the low-gain CCDs.

The calculated energy is biased upwards significantly, and only approaches reality for pulses above 1.5 MeV and DELCO>20. Some of the 1997 cuts were based upon the fit energy of the 2nd pulse, and events were eliminated if the fit energy was above 1.0 or 1.5 MeV. At these energy levels, I suggest that these energy cuts (at least when applied to the low-gain pulse fits) were acting mostly like a prescalar, preferentially eliminating events with low DELCO. This suggestion assumes that the fitting results would not be too dissimilar given the difference in the treatment of the errors between the 1997 analysis and the one used currently.

Test of selection criteria – How much real signal is in the ‘false-positive’ group

In order to check how well the cuts defined above are eliminating fibers without real coincident 2nd pulses, we look at the high-gain CCD pulse fitting. We will document the efficiency of the high-gain CCDs in a later section, but assuming that they work at least as well as the low-gain CCDs, they can tell us something about the reliability of our selection criteria. If fiber selection criteria were valid, then there should be no good two-pulse fit of the selected kaon fibers in the high-gain CCDs when epi_tg=0. (Recall that we select kaon fibers by insisting that the muon track was at least 5 mm away from the nearest corner of the kaon fiber. This should eliminate all ‘vertex’ fibers.) We find that 20% of the fibers that supposedly had no real pion energy but pass the low-gain CCD two-pulse cuts pass a set of similar cuts on the high-gain CCD pulses.

Since this is significantly larger than would be expected if the false-positive probability were random, it implies that there is a relatively minor background of vertex fibers (or Km2g processes or accidentals, etc.) remaining after the setup-cuts. Another interpretation that might be more problematical is that some false-positives are caused by a fluctuation in the actual pulse coming through the fiber-phototube-electronics sequence, which was then correctly encoded in the CCDs, and therefore the fluctuation was seen in both high-gain and low-gain CCD channels. Nevertheless, I don’t think this is a large enough correlation to change the interpretation of the results, so far.

Low-gain fitting efficiency as a function of kaon energy and DELCO

As mentioned previously, we expect the two-pulse fitting probability to vary as a function of the energy of the two pulses and as a function of the time-difference between them. We use the set of cuts defined above, and to get to a low background level, choose DELCOFITCUT to be 4ns. Fig. 5 is a scatter diagram of the distribution of the first pulse energy (abscissa, in MeV) vs. the DELCO (ordinate, in ns).

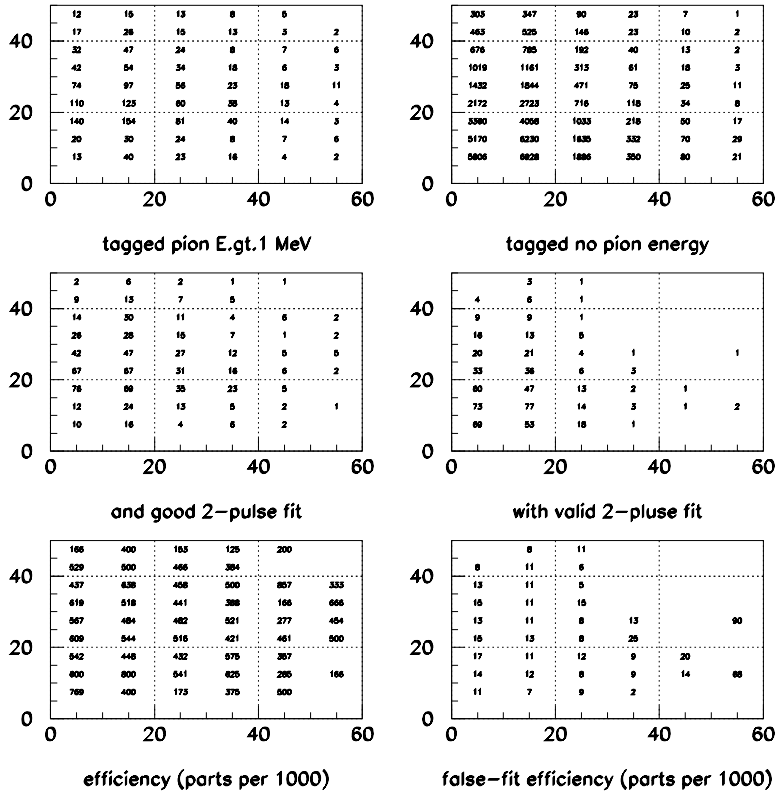


Fig 5. Plots of kaon energy (abscissa, in MeV) vs. DELCO (ordinate, in ns). Left column: fibers which were tagged as having a kaon and a pion with at least 1 MeV in the same low-gain multiplexed channel. Right column fibers in which only a kaon fiber was present.

Top rows: kaon energy vs DELCO; Middle row: a subset of the top row in which the low-gain pulse fits were satisfied; Bottom row: the ratio of the second row to the first row, expressed in parts per 1000.

Examination of this figure shows that the variation of pulse-finding efficiency at a threshold of 1 MeV in the low gain CCDs is a slow function of kaon energy (the lower, the more efficient), and of DELCO (the higher, the more efficient). The efficiency is ~49% for these tagged events. The false-fit efficiency is about 1.2%.

Consistency check on low-gain CCD efficiency used to develop a method for testing High-Gain CCD performance

In the next section, we will study the high-gain CCD performance. When we do this, we have no independent method to test the high-gain efficiency, simply because the fibers are not-multiplexed and, for a sample of pure kmu2 decays, the only way to determine if a ‘pion’ pulse came after the kaon pulse is to use the CCDs. However, if an event was properly reconstructed, and the vertex correctly determined, then the UTC track information extrapolated into the kaon fibers can theoretically determine if a second pulse should or should not have been there.

We can test this methodology by examining the low-gain CCD efficiency by studying kaon-fibers in which none of the other multiplexed fibers had a pulse. In this case, a second pulse should be present only when the muon passed through the kaon fiber. Then we use the UTC trajectories to reconstruct the expected energy distribution deposited by the muons. We then can calculate the CCD pulse-finding efficiency with this ‘extrapolation’ method. We then can compare the efficiency of the low-gain CCDs using the ‘extrapolation’ method with the efficiency done with the previously described ‘tagged’ method.

We used the same setup cuts as described previously. However, instead of applying cuts (a).and.(b).or.(b')) described above, we select fibers that are 1) reconstructed as kaon fibers; 2) which is not the vertex fiber; 3) are between the vertex fiber and the exit point; and 4) have an expected path-length determined from the UTC extrapolation of at least 4mm. For this study, we have eliminated the vertex fiber since we can not reconstruct the actual muon path in the k decay fiber. We also eliminate kaon fibers that are on the other side of the vertex, since the muon should not have passed through them. The expected path-length criterion allows us to predict the muon energy distribution and should eliminate many of the fibers that the extrapolated track actually missed.

We find that 1399/8827 (15.8+-0.4)% kaon fibers passing the 'extrapolation' cuts with $4 < \text{DELCO} < 50$ and $ek_tg < 60$ pass the low gain CCD cuts ($\text{DELCOFITCUT} < 4$, and the rest of the fit cuts defined previously). Using the 'tagged' fibers (effective energy threshold for being tagged is ~ 0.2 MeV), we find 809/3869 (20.9+-0.7)% pass the same low-gain CCD cuts within the same range of ek_tg and DELCO.

In order to understand these numbers, we need to examine distributions and the biases that the different selection criteria create. We have seen already that the efficiency for getting a successful fit is a function of the energy of the 2nd pulse, the energy of the 1st pulse, and the time difference between them. Thus, we need to understand if there may be differences in these parameters in fibers that are being examined. We show below that the differences in apparent efficiency become very small after factoring out the differences in the distributions.

Fig 6 shows the integrated pion energy distribution for the two samples. For the 'extrapolation' cuts, the pion fiber energy distribution of the pion fiber closest to the vertex is given. Only fibers with an expected range in the fiber from the UTC track extrapolation of at least 4mm is plotted. For the 'tagged' method, fibers that were multiplexed into the same CCD channel as the kaon were examined, and those that were tagged as pions are shown. (Excluded in both cases are pions that were found in the kaon fibers.) The probability distributions show relatively minor differences. The 50% point in the extrapolated sample is at 1.00 MeV, whereas it is at 0.98 MeV in the tagged sample.

Several biases that have not been estimated remain in both of these distributions. The effect of these is likely small. Both suffer from the ~ 0.1 - 0.2 MeV energy threshold for the ADC/TDC to define hits. The 'extrapolation' method uses the pion energy in the pion closest to the vertex, when the UTC extrapolation predicts a range of at least 4mm in the fiber. However, we actually need the energy distribution in the kaon fibers, which will be more than ~ 5 mm further along the UTC track. This effect should slightly soften the expected energy distribution in the 'extrapolation' sample. This method also ignores fibers that were entirely missing. The expected range and energies are examined in 'pion' fibers; no range is presently calculated in fibers that were not classified as either kaons or pions. This also would tend to make the average energy distribution in the 'extrapolation' sample slightly softer.

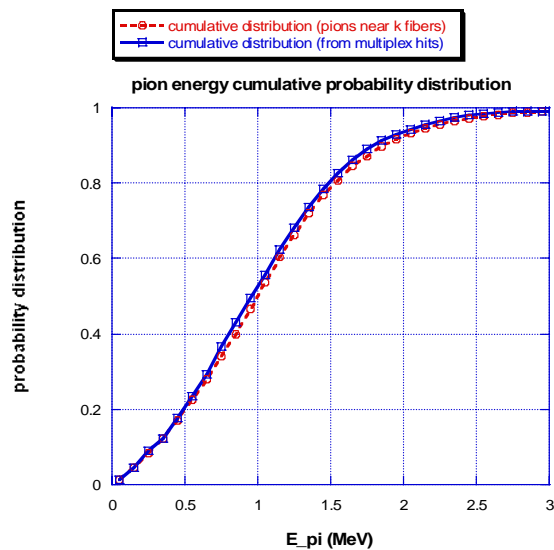


Fig 6. Integrated pion energy distributions. In red is the distribution of energies expected in the kaon fibers which fall on the UTC track and have an extrapolated range of at least 4mm ('extrapolation method'). In blue is the distribution of energies found in the 'tagged' method.

Examination of the DELCO distribution shows no significant difference between the two samples. However, the ek_{tg} distributions are very different. (See Fig 7.) This difference stems from the bias of which kaon fibers are included by the differing selection criteria. In the tagged sample, we eliminate any kaon fiber with any edge closer than 5mm from the UTC track. This eliminates most of the fibers including and near the vertex; and the expected dE/dX of fibers near the vertex is expected to be highest. In the extrapolation sample, the vertex fiber has been eliminated, but kaon fibers on the UTC track beyond the vertex are included.

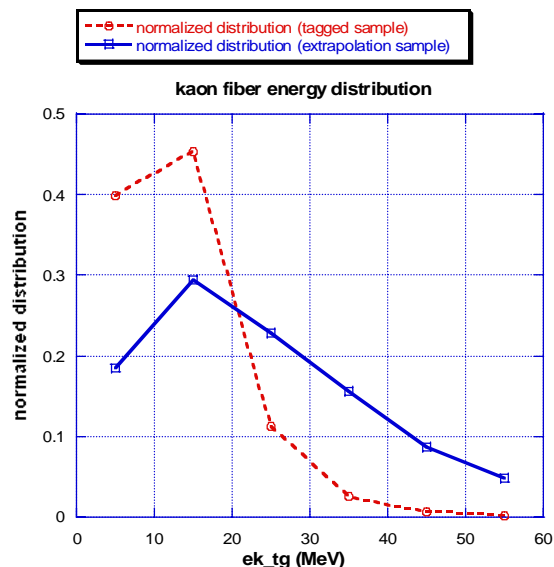


Fig. 7. Energy distribution for kaon fibers selected in the tagged sample (red) and extrapolation sample (blue).

We examine if this is primarily responsible for the differences in the overall efficiency of the low-gain CCD cuts between the two samples. Results are given in Table 2.

Ek_tg (MeV)	Efficiency of low-gain CCD cuts in tagged sample	Efficiency of low-gain CCD cuts in extrapolation sample	Difference in units of standard deviations
0-10	.257±.013	.283±.013	-1.4
10-20	.194±.010	.197±.009	-0.2
20-30	.124±.017	.120±.008	+0.2
30-40	.120±.035	.078±.007	+1.2
40-50	.083±.059	.066±.009	+0.3
50-60	.125±.125	.057±.012	+0.5

Table 2. A check on the efficiency of the low-gain CCD pulse fitter using the set of cuts described above, comparing the ‘tagged’ sample with the ‘extrapolation’ sample. The efficiencies are integrated over $6 < \text{DELCO} < 50$ and the (unmeasured) energy of the 2nd pulse.

There is no significant difference in the low gain CCD cut efficiency in the two samples, when one takes into account the differing ek_tg distributions. This agreement gives us confidence that the ‘extrapolation’ method may be used to study the high-gain CCD performance.

Tests of Performance (High Gain CCDs)

Now, let us turn our attention to the non-multiplexed high gain CCD analysis. As we have said before, there is no direct way to determine the efficiency because there is no way to tell if a pion was in the same fiber as a kaon except by examination of the extrapolated UTC track or the CCD analysis. However, we can use the same setup cuts as used before to test the high-gain CCDs. And, fortified by the agreement in the low-gain CCD cut efficiency between the ‘tagged’ and the ‘extrapolation’ samples, we can be more confident in using the ‘extrapolation’ method in exploring the high-gain CCD fitting efficiency.

Some have suggested that we can test the pulse finding efficiency by artificially ‘adding’ the digitized information of two separate high-gain channels (one found to be a kaon and the other found to be a pion from the ADC and TDC information), and then fitting the resultant pulse. This is an interesting idea, and I welcome any interested party to undertake this study.

Method

To the extent that the setup cuts eliminated fibers that had a coincident particle, we examine the kaon fibers. Analogous to the low-gain cuts, the following cuts are applied:

$\text{doublprob} > 0.001$ (probability of high-gain two-pulse fit > 0.001);
 $\text{doublampp} > 0$ (amplitude of 2nd pulse > 0);
 $\text{doubltimk} > -5$ (time of 1st pulse $> -5\text{ns}$);
 $\text{nonzbins} > 2$ (number of bins used in fit > 2);
 $\text{abs}(\text{doubtimp} - \text{doubltimk} - \text{tpi} + \text{tk}) < \text{DELCOFITCUT}$ (the difference between the two fit times and the expected time difference $< \text{DELCOFITCUT}$; and
 $\text{singlprob} < \text{doublprob}/10$ (the high-gain CCD single fit probability is at least a factor of 10 lower than the double-fit probability).

Results

We find that the ‘false-positive’ probability is about 1.4% for $\text{DELCO} > 15\text{ns}$, using the cuts analogous to the low-gain cuts described before, and $\text{DELCOFITCUT} < 4$. Checking the cuts used in the 1997 analysis ($\text{DELCOFITCUT} < 10$, and $\text{singlprob} < 0.001$ that replace two of the analogous cuts above), the ‘false-positive’ rate is 0.5%.

Now, we examine those kaon fibers that were found to be on the UTC track with extrapolated range $> 4\text{mm}$. The vertex fiber is not included. Results are shown in Fig 8.

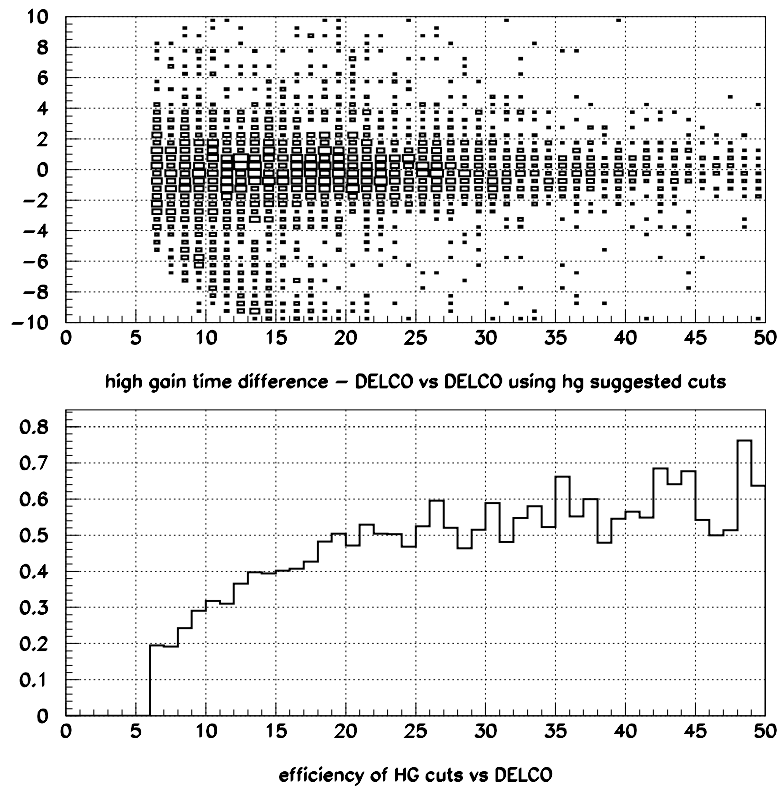


Fig 8. Pulse time difference $-\text{DELCO}$ vs DELCO for high-gain CCD pulses, and the efficiency of the high-gain CCD cuts. The band of events near $(10, -6)$ are presumably mostly due to misreconstructed pulses or false-positives.

The efficiency using DELCOFITCUT=4 is 47% for DELCO>15 ns. We expect that the efficiency will vary as a function of both DELCO and the energy of the kaon similar to that found in the low-gain CCD pulse analysis. A tabulation of this dependence is shown in Fig 9.

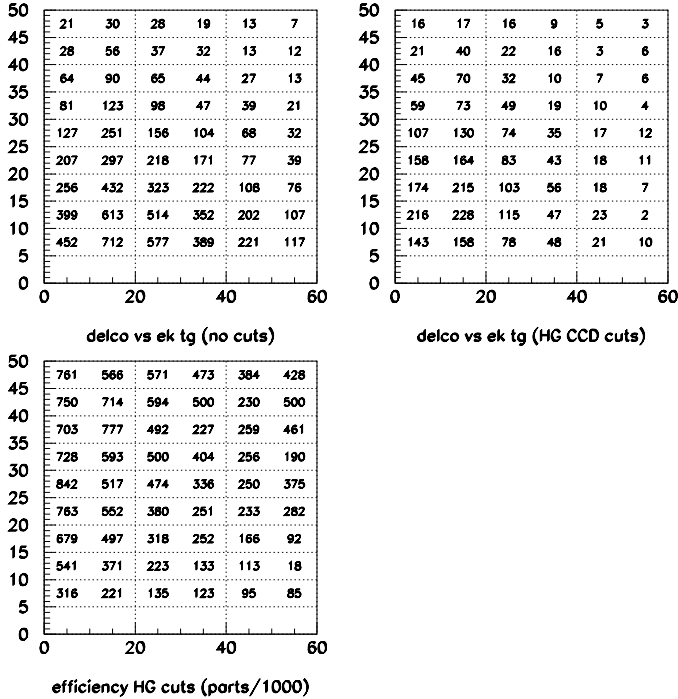


Fig 9. Plots of Ek_tg (abscissa) in MeV vs. DELCO (ordinate) in ns. Upper left shows the number of fibers examined; upper right gives the number that pass the set of high-gain CCD cuts as described in the text. The lower left gives the efficiency of each bin, expressed in parts per 1000. This shows that the efficiency approaches ~75% for low kaon energy and high DELCO.

Now, using the information in Fig 6 of the expected pion energy distribution in the extrapolation sample, we can transform the efficiency plot into a plot of the effective energy threshold of finding a second pulse. This is shown in Fig. 10.

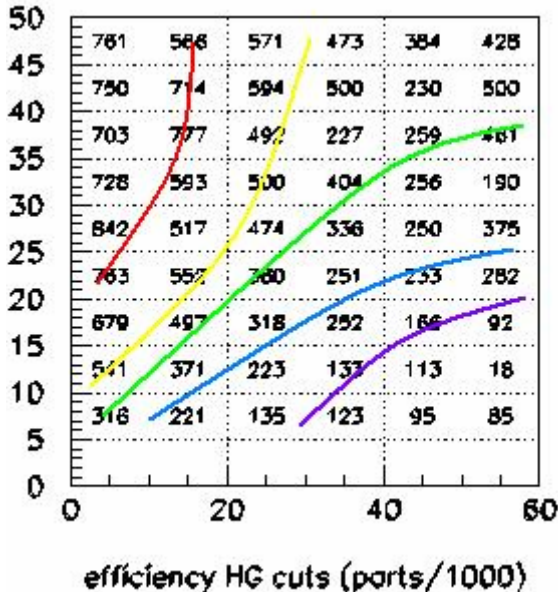


Fig 10. Approximate thresholds for finding a second pulse in MeV in the high-gain CCDs plotted in the space of abscissa Ek_tg and ordinate DELCO. Contours are ~0.75 MeV (red); ~1.0 MeV (yellow); ~1.25 MeV (green); ~1.5 MeV (blue); and ~1.75 MeV (purple). The lowest thresholds are at high DELCO and low Ek_tg.

Using the extrapolation method, we can compare the results of pulse-fitting in the high-gain CCDs with the low-gain CCDs. We use the same set of cuts for each as listed previously. Recall that in the ‘extrapolation’ method, we have no direct determination of the energy of the 2nd pulse.

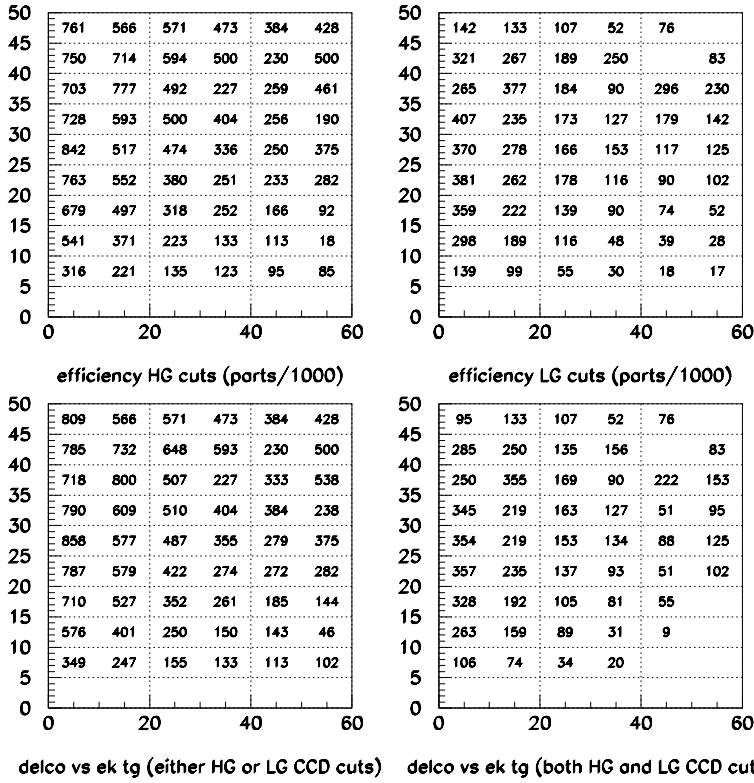


Fig 11 shows plots of the efficiencies (in parts per 1000) of the high-gain CCDs and the low-gain CCDs. Ek_tg (abscissa) vs. delco (ordinate). Also shown is the efficiency of either cut being satisfied (lower-left) and the efficiency of both high-gain and low-gain CCD cuts being satisfied. The efficiency indeed goes up when either high- or low- gain CCD cuts may be used, but the ‘false-positive’ rates will also be higher. This is shown in Fig 12.

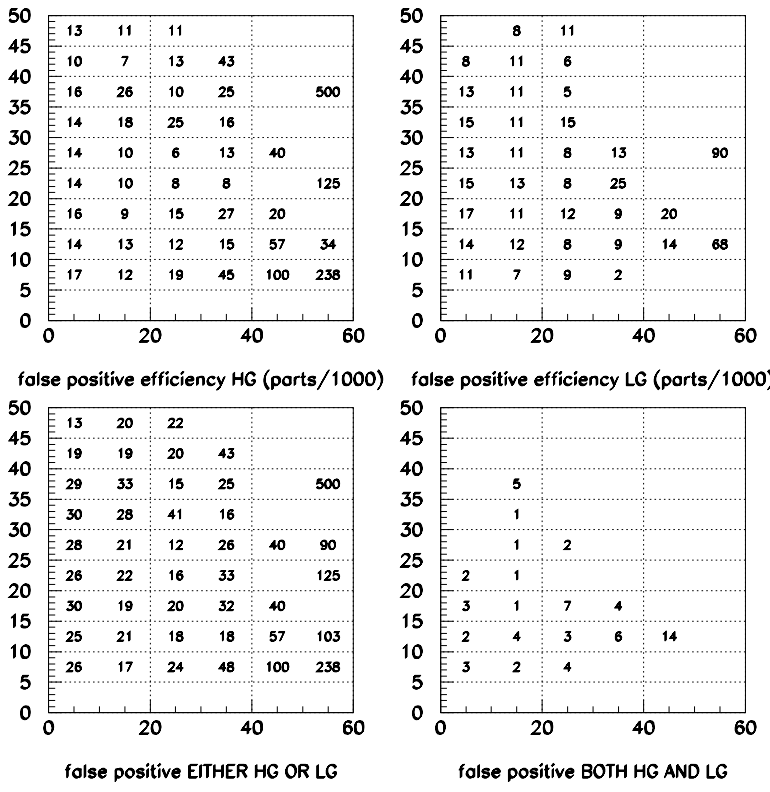


Fig 12. False positive fit efficiencies in parts per 1000 for: (UL) high-gain CCDs; (UR) low-gain CCDs; (LL) either high-gain OR low-gain CCDs; (LR) high-gain AND low-gain CCDs

We find that the high-gain CCDs have successful fits about 2 – 3 times as often as that of the low-gain CCDs.

We can examine the energy of the 2nd pulse in the high gain CCDs. This is shown in Fig. 13. It is clear that the same kind of bias occurs in the high-gain CCD pulse fits as was seen in the low gain CCD pulse fits on tagged samples shown in Fig 4. One would expect a bias to occur simply as a consequence of the efficiency of finding a 2nd pulse varies as a function of DELCO as well as the energy of the 2nd pulse. However, from the number of events with the derived energy of the 2nd pulse more than about 3 MeV, it seems like there is a bias in the reconstructed energy as well.

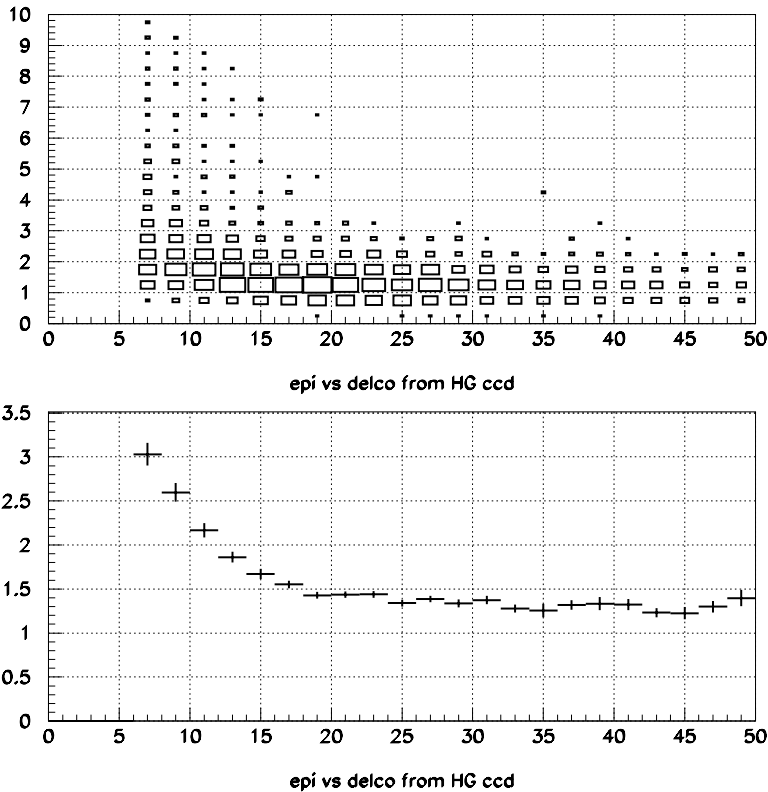


Fig 13. DELCO (abscissa) in ns vs. reconstructed energy of the second pulse (ordinate) in MeV from the high-gain CCDs. Top plot clearly shows the energy distribution has a tail in which the 2nd pulse energy has been overestimated in the CCD pulse fitting routines. The profile plot at the bottom shows the gradual leveling off of the 2nd pulse energy. A linear fit to epi between $20 < \text{DELCO} < 50$ gives $(1.54 \pm .05) - (.0061 \pm .0016) * \text{DELCO}$.

It seems that an application of a reconstruction threshold of 1.0 or 1.5 MeV in the high-gain CCDs, as was done in the previous analyses, is likely not really applying a cut at these thresholds when DELCO is less than ~20ns.

What improvements can be made?

So far, we have examined the CCD fitting results based upon the PASS2 code that was constructed in late 2004. We have found that the pulse fitting works in general, but it has significant inefficiencies. It may be worthwhile to study if some set of changes in the fitting algorithm might allow significant improvements.

As described previously, the errors used in the MINUET minimization routines are of the form $a + b * \text{sqrt}(d_i)$ where d_i is the CCD pulse data (in raw counts) in time bin i ; values of the parameters a and b are different for high-gain and low-gain, but all target fibers use the identical parameters. We can compare the probability distributions of all fibers to understand if there might be significant fiber-to-fiber differences. Fig. 14 shows the average of the low-gain single pulse probability distributions for fiber numbers 200-400. It is very clear that there are large differences in the average likelihood distributions. Distributions of the averages in high-gain channels show similar variations.

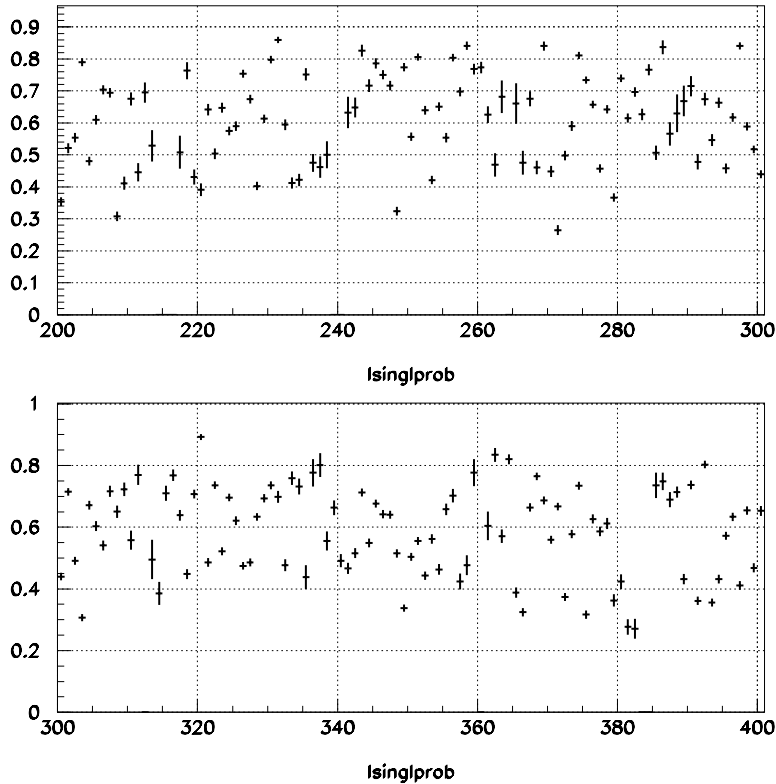


Fig. 14. Average of the low-gain single pulse likelihood distributions for fibers 200-300 (top) and fibers 300-400 (bottom).

We can check to what extent this variation in the low-gain channels comes from pulse fluctuations in the fibers or from the CCDs by grouping the averages into the multiplexed CCD units. This is shown in Fig 15. It is clear that a large part of the variation from fiber to fiber originates from the variations in common to individual CCD channels. This could originate from common noise feeding into the CCD units (like, for example, from the NIM summer units in which the individual signals are added) or from differences in the noisiness within individual CCD channels.

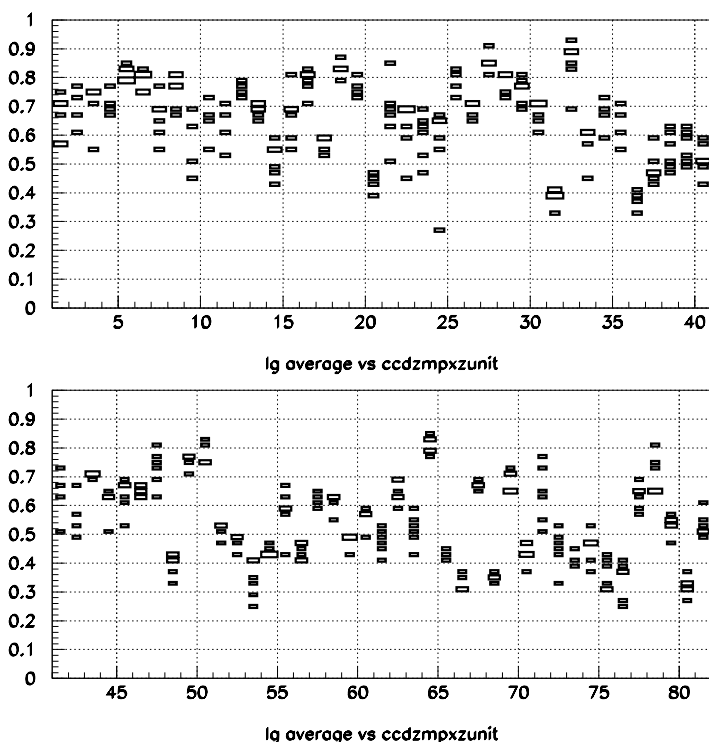


Fig 15. The average of the low-gain CCD likelihood distributions grouped into the individual low-gain CCD channels. Each unit sums 3 to 6 individual fibers. It is obvious that there is a significant correlation of the individual fiber averages with CCD unit.

To gauge the impact of installing individual error factors for each fiber, the same km21 data was run through the PASS2 code with 3 different values of the parameter \mathbf{a} for the constant term in the errors input to the minimization. Then, for each fiber (and each gain), the average values of the probability distributions were fit to arrive at a predicted value of \mathbf{a} for each fiber. The goal was to equalize the average value of the probability distribution for all fibers. After fitting, the average and standard deviations of the distributions of \mathbf{a} were 1.00 ± 0.51 for low-gain, and 1.27 ± 0.67 for high-gain. Next, the PASS2 code was run again, where values of \mathbf{a} were read in for each fiber and both gains (the allowed range was truncated between 0.5 and 4.0). Finally, we checked to see if there was any effect in how well we are able to fit the data.

Table 3 reproduces a part of Table 1, using $\text{DELCOFITCUT} < 4$ and $\text{DELCO} > 15$ on the tagged sample of low-gain CCD fits, and the identical set of cuts. We find a significant, though undramatic, improvement in the results.

	Errors in fit the same for all fibers	Errors in fit different from fiber to fiber
Epi=0 (false positives)	.013	.014
Epi 0 to 0.5 MeV	.034	.040
Epi 0.5 to 1.0 MeV	.132	.184
Epi 1.0 to 1.5 MeV	.309	.358
Epi 1.5 to 3.0 MeV	.602	.635

Table 3. For 'tagged' events, the effect of using individual fiber constant terms in the fit rather than one parameter for all low-gain channels.

Now, we look at the ‘extrapolation’ method to see the effect of applying different constant terms to each individual fiber. Integrating over ek_{tg} and DELCO, the efficiency for satisfying the low gain cuts was 0.154 with the original method. When individual fiber constant terms were used, the efficiency became 0.186, confirming the trend given in Table 3 for the low-gain fits.

Results on the high-gain efficiencies were disappointing, however. With uniform constant terms, the efficiency was 0.335; with individualized constant terms, the efficiency became 0.287. Upon further examination, we find that the ‘false-positive’ probability in the high-gain CCDs went from 1.5% to 0.8% with our standard set of cuts. It is possible that main reason for these changes was that the overall average of the constant term in the error parameterization went from 0.74 to 1.27 for the high-gain channels.

We can modify the set of high-gain cuts to recoup the decrease in efficiency. For example, leaving all other cuts the same and changing ($singlprob < doublprob/10$) to ($singlprob < doublprob/4$), the false positive probability goes from 0.8% to 1.2% and the extrapolation method efficiency changes from 0.287 to 0.337, about the same as obtained previously.

Conclusions and Suggestions for further work

A method utilizing the known energy and times of target pulses that arrive in the low-gain multiplexed CCD channels has been developed. Using this ‘tagged’ method, we have been able to deduce an efficiency calibration in the low-gain CCD channels. We verify that we can get consistent results between the ‘tagged’ method and an ‘extrapolation’ method which uses a distribution of expected 2nd pulse energy, first pulse energy, and the time between them based upon the extrapolated UTC track. Finally, we use the extrapolation method to get an efficiency distribution of the high-gain CCD pulse analysis.

We find that the resulting efficiencies are poor for small DELCO and/or large first-pulse energies, and a threshold of $\sim 3/4$ MeV is only achieved when the first pulse has less than 20 MeV and the DELCO is more than 20ns. We propose a set of cuts that seems to achieve the optimum efficiency consistent with a low expected background rate from ‘false-positives’. From this study, it appears that the efficiency of the CCD system will be very poor in finding 2nd pulses with less than several MeV of energy if one attempts to examine the region of $DELCO < 6ns$, and is poor, in fact, even in regions that were used in previous studies. Since the fitting method is different than that used in prior analysis, we do not know if the current technique is better or worse than the one used in prior pnn2 analyses.

We suggest that the cuts developed and the techniques described in this note may be used to ‘guide’ the acceptance/rejection cuts that will be imposed in the 2002 pnn2 analysis.